Articulated and Flexible Multibody Satellite Dynamics Modelling

20th AIAA International Communication Satellite Systems Conference and Exhibit
12-15 May 2002, Montreal, Quebec, Canada

AIAA 2002-2056

ARTICULATED AND FLEXIBLE MULTIBODY SATELLITE DYNAMICS MODELING

P.A. Gili* Associate Professor
M. Battipede† Ph.D. Researcher
R. Ruotolo‡ Assistant Professor
L. Massotti Ph.D. Student
Aeronautical and Space Department, Politecnico di Torino
Turin - ITALY

Abstract. This paper is concerned with the derivation of the equations of motion for a maneuvering flexible satellite orbiting around the Earth. The structure is assumed to undergo large rigid-body maneuvers and small elastic deformations. The mathematical model is worked out in two levels: in the first one attention is focused on the effects of the rigid dynamics on the flexible motion, while in the second one the reciprocal influence is evaluated.

The satellite is provided with flexible solar arrays linked up with the main body with torsional and bending articulations: the mathematical model also considers hinges compliance, when the appendages are blocked in the desired position. Different rotational maneuvers are simulated and numerical results highlight the limitation of the first level modelization, which can be used with confidence for structural analysis, but results inadequate for flight dynamics and control applications.

List of Symbols

$\mathbf{a}$	point P position vector
D	Integration domain
$\mathbf{f}$	Force vector per unit of volume
F	Reference frame
G	Universal gravitational constant
k	Hinge stiffness
$[J]$	Inertia matrix
$[L_{BO}]$	rotating matrix from F_B to F_O
$[L_{OP}]$	rotating matrix from F_O to F_{pi}
M	Gravity-gradient torque
m	Mass
n	Constant orbital rate
$m_\oplus$	Earth's mass
P	Nominal point on a panel
$\mathbf{q}$	Modal coordinate vector
q_j	Generic Lagrangian coordinate
Q_j	Lagrangian forcing vector
$\mathbf{r}$	point S position vector
$\mathbf{R}$	CG satellite position vector
S	Nominal point on the bus
T	Kinetic energy
U	Potential energy
V	Translational velocity vector
$\mathbf{w}$	point P elastic displacement vector
W	Virtual work
$\boldsymbol{\alpha}$	Euler angle vector
β	Panel position angle referred to (x_B, y_B) plane
δ	Panel rotation angle around y_B axis
η_x, η_y	Point P coordinates in a local reference plane
ϕ, θ, ψ	Euler angles
μ	Gravitational parameter of the Earth
$\boldsymbol{\omega}$	Angular velocity vector of body reference frame
$\boldsymbol{\sigma}$	Hinge compliance vector
$\triangle$	Variation with respect to a nominal condition

Subscripts

0	Undeformed condition
a	Appendage
b	Main bus
B	Body reference frame
$bend$	Bending
e	Elastic
F	Force
g	Gravitational
H	Compliance
I	Inertial reference frame
l	Left
M	Moment
$tors$	Torsional
Q	Bending
r	Right

*AIAA Member
†AIAA Member
‡AIAA Member

Introduction

In the last two decades, the problem of vibration assessment and control of flexible spacecrafts has become increasingly important. As a matter of

fact, with the sudden development of satellite communications, the most relevant problem is to establish whether the structure is able to support stress concerning the orbit injection, orbital or station-keeping maneuvers and flexible appendages deployment. Moreover, structure response to different inputs (slewing maneuvers, impacts with micro meteorites, etc.) must be assessed in operative conditions: vibrations suppression becomes fundamental to observe more and more accurate aiming target for antennas (for telecommunications) and cameras (for survey, weather forecast and military aims). Some studies carried out by NASA[1], involve experiments concerning the control problem of flexible bodies carried by a shuttle in a geocentric orbit; other missions involve Earth-based laboratory simulations of similar experiments. Since the space environment is hardly reproducible in laboratory and deploying an unproven system could be disastrous, mathematical modeling and computer simulation are valuable to ensure the success of future missions or future designs.

In the past, the mathematical model of space structures was tackled with different approaches. Early spacecraft models were mostly rigid[2],[3],[4], or modeled as a number of interconnected rigid bodies. Afterwards a formalism was developed to describe the behaviour of structures in which some of the interconnected bodies were flexible[5],[6],[7]. As an alternative, other methods based on lumped schemes were applied, such as the component-mode synthesis or the substructure synthesis[8],[9], where structures were modeled as a collection of substructures, each one represented by a limited number of degrees of freedom.

Recently the massive employment of Finite Elements codes has produced numerous papers dealing with stress in articulate flexible bodies[10], but this papers estimate vibrational motion referred to the unperturbed state which is fixed in the inertial reference frame.

Refs. [11] and [12] address the problem of a single-axis rotational maneuver and simultaneous vibration suppression of a spacecraft, consisting of a rigid core with a number of flexible vibrating booms. However the orbital motion is not considered.

Meirovitch et al.[13] derived the equations of motion for a maneuvering flexible spacecraft both in orbit and in an Earth-based laboratory. They proposed a perturbation approach to decouple the rigid motion from the flexible one: elastic vibrations equations turn out to be linear with time-dependent coefficients, while the forcing term is dominated by the rigid body motion, described by a set of nonlinear ordinary differential equations. Assumption concerning this hybrid model is that small elastic deformations do not affect the rigid body behavior, however no evidence are shown to support this hypothesis.

Another point is that, when dealing with complex structures, rarely the compliance of deploying hinges is taken into consideration for dynamics modeling. Generally this problem is addressed only from the kinematic point of view, as in Ref. [14], where the solar arrays deployment phase is simulated, or in Ref. [15], where an attitude control system is applied to the mechanical arm.

In this paper two mathematical models have been worked out. The first model reminds of the Meirovitch 's hybrid model: the rigid body equations of motion are considered as an independent set and written according to the classical nonlinear formulation, which allows the description of the rigid body wide motions. At the same time a set of linear differential equations is used to describe the flexible appendages elastic displacements from the equilibrium configuration. The forcing term of the linear system is calculated step by step by integrating the equations of motion of the rigid body.

The second one is obtained through the Lagrange equations applied to the whole system, which means that the contribution of each component is summed for the calculation of the kinetic and the potential energy. This method leads to a nonlinear, time-varying, differential system of equations, with couplings between rigid and flexible motion variables. This model can be used to assess the reciprocal effects of the two motions and for this reason has been named *fully-coupled*.

Effects of the interaction between rigid and flexible motions can be observed from the time histories concerning standard maneuvers. Moreover, the system is provided with deployment hinges that have an intrinsic compliance, so that the bending and torsional deformations of the panels are coupled with motion caused by hinges, which may change modal parameters.

Attention is focused on the maneuver effects on solar arrays: it is emphasized how the behavior of flexible structures is affected by centrifugal forces and gravitational moments, while the degree of accuracy of the simplified hybrid mathematical model is evaluated by means of numerical comparisons.

The paper is organized as follows: firstly, a short description of the satellite geometry is provided. In the second and third sections the equations of motion for both hybrid and fully-coupled model are derived. Numerical results are reported in the last sec-

tion, for different maneuvers concerning rotations in roll and pitch.

Satellite geometry

The satellite which was considered for simulations is shown in Fig. 1: it has a very simple geometry, but it contains all the structural elements which characterizes scientific and telecommunication satellites.

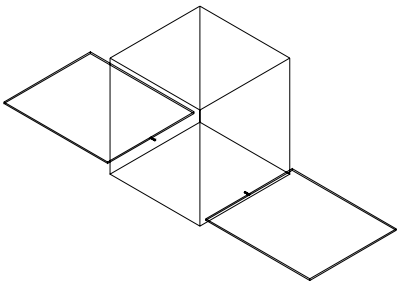

Figure 1: Satellite geometry

The basic assumptions are the following:

- the main body is rigid and modeled with a concentrated mass scheme. Data concerning the main body mass distribution and inertia have been retrieved in the available literature;
- solar arrays are symmetrical and flexible; they are made up of photovoltaic cells and have been designed with reference to the B.O.L. power, typical of a medium size satellite. The elastic motion is measured relatively to the rigid body frame and perpendicularly to the undeformed plane;
- solar arrays are linked up with the main body with torsional and bending articulations, which allow them to be deployed and oriented. When appendages achieve the desired configuration, they are constrained by a blocking device, which is supposed to be pliable. Hinges are supposed concentrated in two points, one for each array.

It is convenient to refer the motion of the satellite to a body reference frame F_b (x, y, z), with the origin in the centre of gravity of the whole system. The motion of the reference frame is characterized by six degrees of freedom; the elastic motion is measured relative to the rigid frame and is characterized by an infinite number of degrees of freedom.

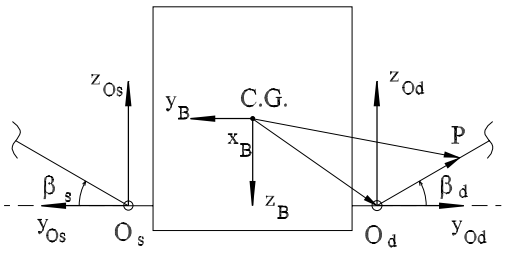

Figure 2: Reference frames

Hybrid mathematical model

This model is based on the assumption that rigid and flexible motions can be decoupled: as a matter of fact the rigid body motion trigger off solar panels vibrations, but this effect is supposed to be uninfluential on the rigid body motion. According to this hypothesis, equations can be devided into two sets: the first one describing the rigid body dynamics and the second one for the flexible motion.

The rigid body motion is described by a set of 9 nonlinear differential equations:

- orbital trajectory equations;
- moment equations;
- kinematic equations.

Orbital trajectory equations can be written with respect to a perifocal frame[16], which coincides with the Earth Centered Inertial (ECI) frame for a circular orbit. Solving the classical two body dynamic problem[14], the trajectory equations results:

$$\ddot{\mathbf{R}} + \frac{\mu}{|\,\mathbf{R}\,|^3}\mathbf{R} = 0 \qquad (1)$$

where μ is the gravitational parameter of the Earth-satellite system and $\mathbf{R}$ is the CG satellite position, measured with respect to the perifocal inertial frame origin. This vectorial equation describes the motion of the CG satellite along a circular orbit.

Moment equations are derived through the angular momentum conservation principle:

$$[J]\dot{\boldsymbol{\omega}} + \tilde{\boldsymbol{\omega}}[J]\boldsymbol{\omega} = \mathbf{M} + \mathbf{T} \qquad (2)$$

where $\mathbf{M}$ is the gravity gradient acting on the satellite along the orbit. Being n the orbital angular velocity and $\mathbf{a}_3$ the local body axis pointing towards the Earth, $\mathbf{M}$ can be written as follows [14]:

$$\mathbf{M} = 3n^2 \mathbf{a}_3 \wedge [J] \cdot \mathbf{a}_3 \tag{3}$$

$\mathbf{T}$ is the control torque vector, which is provided by proper thrusters, conveniently placed on the inertia main axes.

Finally, kinematic equations can be written in the following vectorial form [14]:

$$\dot{\alpha} = [E(\phi, \theta, \psi)]\, \boldsymbol{\omega} + n\mathbf{F}(\phi, \theta, \psi) \tag{4}$$

Solving these equations in the time domain, the time histories of the rigid body motion state vector can be obtained and used to evaluate the forcing terms of the panels flexible motion.

As far as elastic deformations are concerned, a Finite Element Method (FEM) linear model of solar arrays was worked out. Each panel is divided into 32 rectangular plane elements with one of the shorter boundaries hinged to the central body. After panel deployment and orientation, hinges are blocked in the nominal position, which means that solar arrays should be considered as cantilevers. However, as hinges are torsionally pliable, also the points belonging to the constrained boundary may deviate from the equilibrium position.

Node displacements are measured in local frames F_p $(O_p\, x_p\, y_p\, z_p)$ with $p = 1...45$, as shown in Fig. 3 for the right panel.

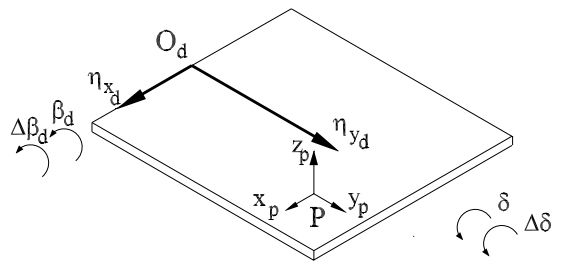

Figure 3: DOF and local frames for the right panel

Each point P has coordinates η_{xp} and η_{yp} referred to the middle point of the hinged boundary. Two reference frames are introduced to account for the torsional and bending degrees of freedom of the hinges. The solar arrays are oriented towards the Sun and the declination angle relative to the x body axis is identified by δ. The model also provide the possibility to deploy the panels in different equilibrium positions through the bending angle β. Values of this angle different from the null value cause variations of the inertia term I_{zz}: its decrease implies low torque maneuvers, with a consequent saving of fuel and decreasing stresses on the structure. The hinges compliance affects the equilibrium configuration with small perturbations denoted with $\triangle\beta$ and $\triangle\delta$ (with subscript l or r respectively for the left or the right panel).

According to the above considerations, the displacement of the generic point P on each panel can be written in the F_{pi} local reference frame as follows:

$$\mathbf{w}_{rel} = \begin{bmatrix} 0 \\ 0 \\ w_{ro} + \triangle\beta\, \eta_y \pm \triangle\delta\, \eta_x \end{bmatrix} \tag{5}$$

where w_{ro} is the elastic displacement in the normal direction w.r.t. the undeformed surface in the local reference frame F_{pi}. The relative velocity vector can be easily derived from equation (5) and both can be expressed in the body reference frameF_B with a simple double rotation, according to:

$$\mathbf{w}_{rel_B} = [L_{BO}]^T [L_{OP}]^T \mathbf{w}_{rel} \tag{6}$$

$$\dot{\mathbf{w}}_{rel_B} = [L_{BO}]^T [L_{OP}]^T \dot{\mathbf{w}}_{rel} \tag{7}$$

In the undeformed configurazion, P can be located through the position vector $\mathbf{a}_B$, expressed in the F_B reference frame as a vector composition:

$$\mathbf{a}_B = \mathbf{O}_B + [L_{BO}]^T [L_{OP}]^T \mathbf{P} \tag{8}$$

where $\mathbf{O}_B$ is the hinge position w.r.t. the system CG in the body reference frame while $\mathbf{P}$ is the distance between the hinge and the nominal point P, in the local reference frame.

Thus, the kinetic energy relative to the flexible motion can be written for each panel as follows:

$$T = \frac{1}{2} \int_{m_a} |\mathbf{V} + \boldsymbol{\omega} \wedge (\mathbf{a} + \mathbf{w}) + \dot{\mathbf{w}}|^2 \, dm_a \tag{9}$$

which accounts both for the rigid body motion and for the elastic deformations, as well as for the hinges pliability. Singular effects can be better appreciated by dividing equation (9) into six terms, according to

a simpler notation:

$$\begin{aligned} T &= \frac{1}{2}\int_{m_a} |\mathbf{V}|^2 dm_a + \\ &+\frac{1}{2}\int_{m_a} |\boldsymbol{\omega} \wedge (\mathbf{a}+\mathbf{w})\,|^2 dm_a + \\ &+\frac{1}{2}\int_{m_a} |\dot{\mathbf{w}}|^2\, dm_a + \\ &+\int_{m_a} \mathbf{V}^T \boldsymbol{\omega} \wedge (\mathbf{a}+\mathbf{w})\, dm_a + \\ &+\int_{m_a} \mathbf{V}^T \dot{\mathbf{w}} dm_a + \\ &+\int_{m_a} [\boldsymbol{\omega} \wedge (\mathbf{a}+\mathbf{w})]^T\, \dot{\mathbf{w}} dm_a \end{aligned} \tag{10}$$

The potential energy is given by the sum of the elastic and gravitational contributions. The elastic potential energy includes both the hinges pliability effect and the panels strain energy:

$$U_e = \frac{1}{2}\,\mathbf{q}_{r,l}^T\,[k]_{r,l}\,\mathbf{q}_{r,l} + \frac{1}{2}\,k_{bend}\,\triangle\beta_{r,l}^2 + \frac{1}{2}\,k_{tors}\,\triangle\delta_{r,l}^2 \tag{11}$$

The gravitational potential energy can be expressed, assuming that the origin of the inertial coordinate system ECI coincides with the center of the gravitational field (the center of the Earth):

$$U_g = -Gm_\oplus \int_{m_a} |\mathbf{R}+\mathbf{a}+\mathbf{w}|^{-1}\, dm_a \tag{12}$$

where G is the gravitational mass constant and $m_\oplus$ is the Earth mass. The magnitude of $\mathbf{R}$ can be considered by far greater than the other terms in the summation; this consideration enables to perform a binomial expansion, which semplifies the previous expression as follows:

$$\begin{aligned} U_g &\cong -\mu\, m|\mathbf{R}|^{-1} + \\ &+\mu\,|\mathbf{R}|^{-3}\mathbf{R}^T \int_{m_a} (\mathbf{a}+\mathbf{w})\, dm_a + \\ &-\frac{3}{2}\,\mu\,|\mathbf{R}|^{-5} \int_{m_a} (\mathbf{R}^T\mathbf{a})^2 dm_a \\ &+\frac{1}{2}\,\mu\,|\mathbf{R}|^{-3} \int_{m_a} |\mathbf{a}|^2 dm_a \end{aligned} \tag{13}$$

It can be noticed that when deriving this expression with respect to the lagrangian coordinates ($\mathbf{q}$, $\triangle\beta$, and $\triangle\delta$), only the second term provides some coefficients in the equations of motion.

Thus, the equations of motion for the flexible body can be derived with the Lagrangian method:

$$\frac{d}{dt}\left(\frac{\partial T}{\partial \dot{\mathbf{q}}}\right) - \frac{\partial T}{\partial \mathbf{q}} + \frac{\partial U}{\partial \mathbf{q}} = Q_Q \tag{14}$$

$$\frac{d}{dt}\left(\frac{\partial T}{\partial \dot{\sigma}}\right) - \frac{\partial T}{\partial \sigma} + \frac{\partial U}{\partial \sigma} = Q_H \tag{15}$$

Their number is given by the expression:

$$\nu\, n \,+\, \mu \tag{16}$$

where $\nu = 2$ is the number of the flexible appendages; n is the number of the modal coordinates used for each panel and $\mu = 4$ represent the hinge pliablility degrees of freedom (2 for each hinge).

In the matrix formulation, the equations of motion can be written as:

$$[M]\ddot{\mathbf{X}} \,+\, [K]\mathbf{X} \,=\, \mathbf{F} \tag{17}$$

This expression does not contain the $[G]$ matrix, which multiplied the vector $\dot{\mathbf{X}}$ in Meirovitch and Quinn's non-linear model[13] and contained the Coriolis' terms. However, analyzing the forcing vector:

$$F \,=\, f(v_x, v_y, v_z, p, q, r, a_x, a_y, a_z, \dot{p}, \dot{q}, \dot{r}) \tag{18}$$

the presence of coupling terms between the rigid body translational and rotational speeds can be noticed. Consequently, the previous equations of motion contain also the rigid body dynamics terms of Coriolis, which act as forcing terms in the flexible body dynamics.

According to this hybrid model, the satellite maneuvers produce tangential and centrifugal forces which excite the elastic motion. However, elastic and rigid motions are not cross-coupled, meaning that elastic displacements do not affect the satellite attitude.

In the modal analysis a proportional structural damping was also considered and for this reason most maneuvers can be performed without the activation of any vibration control device.

Fully-coupled mathematical model

The hybrid mathematical model features a quite accurate description of what happens on the flexible appendages as a consequence of orbital maneuvers. However, the large size of solar arrays and the total absence of aerodynamic damping lead to presume that structurale vibrations might induce perturbations on the motion of the main body center of gravity. Consequently, depending on the extent of these perturbations, the stress field could be affected significantly, since the stress condition is a function of the relative displacement between each point of the flexible panel and the center of gravity. To evaluate these cross-coulpled effects, the equations of motion of the rigid body must be reformulated by means of the Lagrangian approach. For this purpose, the dimension of the Lagrange vector is increased to enclose also the rigid body dynamics

variables contained in vectors $\mathbf{R}$ and ϕ, θ, ψ. Consistently, the kinetic energy expression must contain also the rigid body contribution:

$$T = \frac{1}{2}\int_{m_b} \dot{\mathbf{R}}_b^T \dot{\mathbf{R}}_b dm_b + \frac{1}{2}\int_{m_a} \dot{\mathbf{R}}_a^T \dot{\mathbf{R}}_a dm_a \quad (19)$$

According to Fig. 2 and to motion composition, it can be written:

$$\dot{\mathbf{R}}_b = \dot{\mathbf{R}} + \boldsymbol{\omega} \wedge \mathbf{r} \quad (20)$$

$$\dot{\mathbf{R}}_a = \dot{\mathbf{R}} + \boldsymbol{\omega} \wedge (\mathbf{a} + \mathbf{w}) + \dot{\mathbf{w}} \quad (21)$$

Hence:

$$\begin{aligned} T &= \frac{1}{2} m \dot{\mathbf{R}}^T \dot{\mathbf{R}} + \frac{1}{2}\int_{m_b} |\boldsymbol{\omega} \wedge \mathbf{r}|^2 dm_b + \\ &+ \frac{1}{2}\int_{m_a} |\boldsymbol{\omega} \wedge \mathbf{a}|^2 dm_a + \\ &+ \dot{\mathbf{R}}^T \left\{ \boldsymbol{\omega} \wedge \left(\int_{m_b} \mathbf{r}\, dm_b + \int_{m_a} \mathbf{a}\, dm_a \right) \right\} + \\ &+ \frac{1}{2}\int_{m_a} \dot{\mathbf{w}}^T \dot{\mathbf{w}}\, dm_a + \\ &+ \dot{\mathbf{R}}^T \left(\int_{m_a} \dot{\mathbf{w}}\, dm_a + \boldsymbol{\omega} \wedge \int_{m_a} \mathbf{w}\, dm_a \right) + \\ &+ \int_{m_a} \dot{\mathbf{w}}^T (\boldsymbol{\omega} \wedge \mathbf{a})\, dm_a + \\ &+ \int_{m_a} (\boldsymbol{\omega} \wedge \mathbf{a})^T (\boldsymbol{\omega} \wedge \mathbf{w})\, dm_a + \\ &+ \frac{1}{2}\int_{m_a} |\boldsymbol{\omega} \wedge \mathbf{w}|^2 dm_a + \\ &+ \int_{m_a} \dot{\mathbf{w}}^T (\boldsymbol{\omega} \wedge \mathbf{w})\, dm_a \end{aligned} \quad (22)$$

where

$$\mathbf{S}_0 = \int_{m_b} \mathbf{r}\, dm_b + \int_{m_a} \mathbf{a}\, dm_a \quad (23)$$

is the structure static momentum and m_b, m_a and m are respectively the masses of the core body, the solar arrays and the entire satellite. Furthermore, compacting the quadratic terms in r, the inertial effects of the rigid body dynamics can be singled out:

$$\begin{aligned} \frac{1}{2}\boldsymbol{\omega}^T [J_0] \boldsymbol{\omega} &= \frac{1}{2}\int_{m_b} |\boldsymbol{\omega} \wedge \mathbf{r}|^2 dm_b + \\ &+ \frac{1}{2}\int_{m_a} |\boldsymbol{\omega} \wedge \mathbf{a}|^2 dm_a \end{aligned} \quad (24)$$

where $[J_0]$ is the total inertia matrix of the undeformed structure about point CG.

Similarly, the gravitational term of the potential energy must be riformulated to include the rigid body contribution:

$$\begin{aligned} U_g &= -G\, m_\oplus \left(\int_{m_b} |\mathbf{R} + \mathbf{r}|^{-1} dm_b + \right. \\ &\left. + \int_{m_a} |\mathbf{R} + \mathbf{a} + \mathbf{w}|^{-1} dm_a \right) \end{aligned} \quad (25)$$

Using the same binomial expansion adopted in the previous section, the overall gravitational potential energy turns out to be:

$$\begin{aligned} U_g &\cong -\mu \left\{ \frac{m}{|\mathbf{R}|} - \frac{1}{|\mathbf{R}|^3} \mathbf{R}^T \left(\int_{m_b} \mathbf{r}\, dm_b + \right. \right. \\ &+ \left. \int_{m_a} \mathbf{a}\, dm_a + \int_{m_a} \mathbf{w}\, dm_a \right) + \\ &+ \frac{1}{2|\mathbf{R}|^5} \left(\int_{m_b} 3\, \mathbf{r}^T \mathbf{R} \mathbf{R}^T \mathbf{r} dm_b + \right. \\ &+ \left. \left. \int_{m_a} 3\, \mathbf{a}^T \mathbf{R} \mathbf{R}^T \mathbf{a} dm_a \right) + \right. \\ &\left. - \frac{1}{2|\mathbf{R}|^3} \left(\int_{m_b} \mathbf{r}^T \mathbf{r} dm_b + \int_{m_a} \mathbf{a}^T \mathbf{a} dm_a \right) \right\} \end{aligned} \quad (26)$$

while the strain energy can be still expressed by Eq. (11).

The virtual work is due to external forces, including maneuvering forces. Denoting with $\mathbf{f}_b$ the force vector per unit of volume of the bus and with $\mathbf{f}_a$ the force vector per unit of volume of the appendages,the virtual work can be written as:

$$\delta W = \int_{D_b} \mathbf{f}_b \cdot \delta \mathbf{R}_b dD_b + \int_{D_a} \mathbf{f}_a \cdot \delta \mathbf{R}_a dD_a \quad (27)$$

where D_b and D_a are the domains of the core bus and arrays, respectively.

After performing the real-to-Lagrange coordinates tranformation and the space discretization, the Lagrange's equations can be derived in the form:

$$\frac{d}{dt}\left(\frac{\partial T}{\partial \dot{q}_j}\right) - \frac{\partial T}{\partial q_j} + \frac{\partial U}{\partial q_j} = Q_j \text{ for } j = 1, ..., n \quad (28)$$

with:

$$q = \{R_x, R_y, R_z, \phi, \theta, \psi, \mathbf{q}_l, \mathbf{q}_r, \triangle\beta_l, \triangle\beta_r, \triangle\delta_l, \triangle\delta_r\}^T \quad (29)$$

In a more extended formulation:

$$\frac{d}{dt}\left(\frac{\partial T}{\partial \dot{\mathbf{R}}}\right) + \frac{\partial U}{\partial \mathbf{R}} = Q_F \quad (30)$$

$$\frac{d}{dt}\left(\frac{\partial T}{\partial \dot{\boldsymbol{\alpha}}}\right) - \frac{\partial T}{\partial \boldsymbol{\alpha}} + \frac{\partial U}{\partial \boldsymbol{\alpha}} = Q_M \quad (31)$$

$$\frac{d}{dt}\left(\frac{\partial T}{\partial \dot{\mathbf{q}}}\right) - \frac{\partial T}{\partial \mathbf{q}} + \frac{\partial U}{\partial \mathbf{q}} = Q_Q \quad (32)$$

$$\frac{d}{dt}\left(\frac{\partial T}{\partial \dot{\boldsymbol{\sigma}}}\right) - \frac{\partial T}{\partial \boldsymbol{\sigma}} + \frac{\partial U}{\partial \boldsymbol{\sigma}} = Q_H \quad (33)$$

where $\boldsymbol{\alpha}$ is the Euler angle vector and $\boldsymbol{\sigma}$ is the hinge compliance vector.

The structure of the two sets of equations are similar to that of the hybrid model, meaning that the equations describing the motion of the rigid satellite are still nonlinear ordinary differential equations, while those describing the small elastic displacements of the flexible satellite are linear partial differential equations. However the first set is by far more complex, since the number of terms is increased significantly and individual effects of variables are very hard to single out.

Nevertheless, as will be shown in the next section this approach enable to evaluate and overcome the limitations of the hybrid model.

Results

Results concern three examples of bang-bang maneuvers, performed with the two model decribed above. For each situation four figures are reported, three featuring the comparison of the rigid body variables and one showing the consequent displacements of a point on the tip panel.

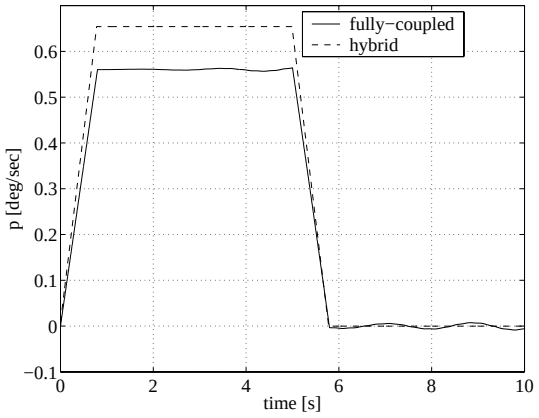

Figure 4: Example ♯1: roll rate

Figg. from 4 to 7 refer to a single pulse maneuver around the x_B axis, which points towards the motion direction. This maneuver is carried out with one pulse spin-up in $t = 0$ *sec* and one pulse spin-down in $t = 5$ *sec*, while the torque supported by the structure during the ignition phase is $T_{max} = 20.63\ Nm$ for 0.8 *sec*. Fig. 4 shows the first bending mode effect on the roll rate: in fact oscillations with a period of less that 2 seconds are clearly visible from the fully-coupled model simulation, in accordance with the modal analysis parameters reported in table 1.

Another substantial difference between the two models consists in the maximum value reached by the roll rate. This phenomenon can be explained

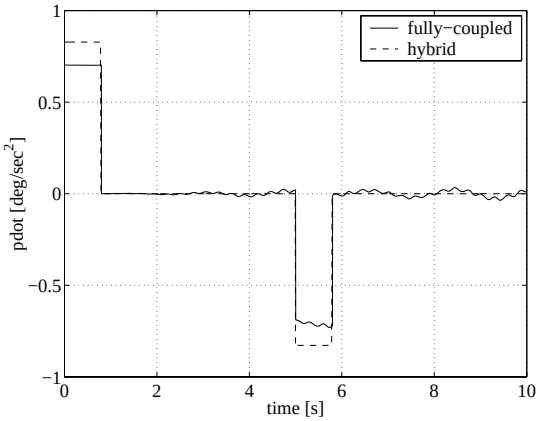

Figure 5: Example ♯1: roll accelation

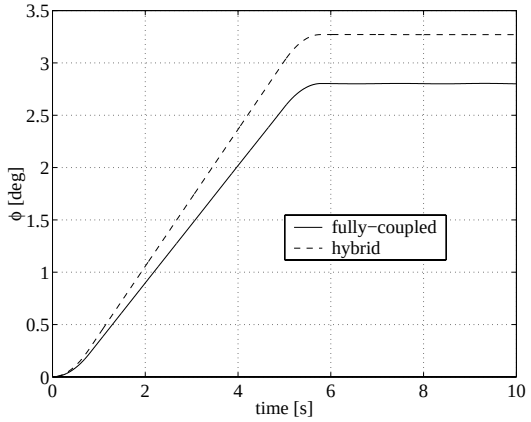

Figure 6: Example ♯1: bank angle

by analysing the terms which make up the inertia matrix: while in the hybrid model there is only a mass contribution, in the fully-coupled model the inertia matrix is augmented by coupling terms between the rigid and flexible body variables, resulting in an overall stiffness increase.

In Fig 5, concerning the roll acceleration, the two peak correspond to the two ignition phases. In the full-coupling model it can be observed how both the first and the second antisymmetrical bending mode affect the roll acceleration trend of the whole body.

Fig 6 shows the difference between the pointing angles ϕ, which is about of $14,4\%$ for the final attitude, reached by the satellite after the maneuver.

Finally, 7 reports the comparison between the displacement evaluated with the two models: the difference arising from the the maximum value of the roll acceleration makes the hybrid results conservative to the stress analysis purpose. In fact peak displacements are over-estimated of about 16%. However this consideration is valid just for the present

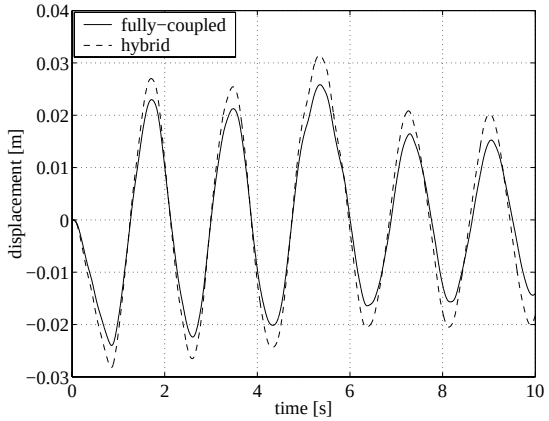

Figure 7: Example ♯1: displacement of a point on the tip panel

example, because this percentage depends on the forcing magnitude.

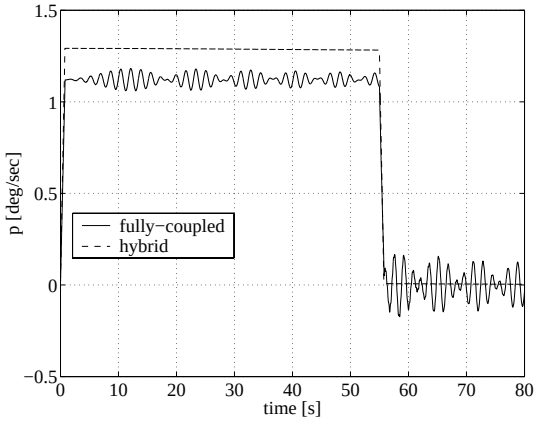

Figure 8: Example ♯2: roll rate

As a matter of fact, Figg. from 8 to 11 refers to the a more demanding maneuver, with the pulse spin-down phase postponed in $t = 55\ sec$ and a maximum torque value of $41,25\ Nm$, namely twice as much as before. The maneuver is also longer and oscillation effects are more evident: high order modes can be seen also in the roll rate trend. The attitude estimation error is decresed as a relative value, but results increased as an absolute value. By analysing Fig. 11, it can be noticed that the peak displacements reached after the spin-down are greater than the spin-up values according to the hybrid model, while feature the same amplitude according to the more reaslistic fully-coupled model.

The last example (Figg. from 12 to 15)concerns a three-pulse maneuver with three pulse spin-up respectively in $t = 1\ sec$, $t = 2\ sec$ and $t = 3\ sec$ and

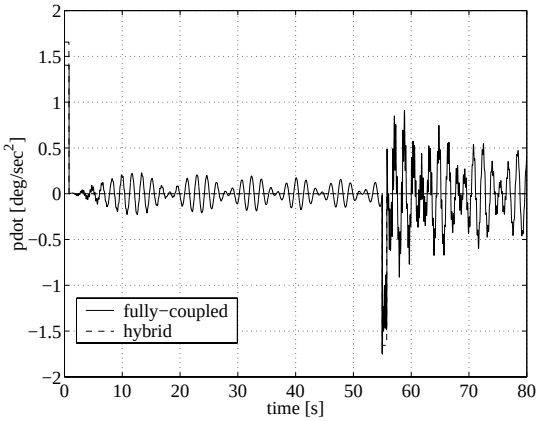

Figure 9: Example ♯2: roll accelation

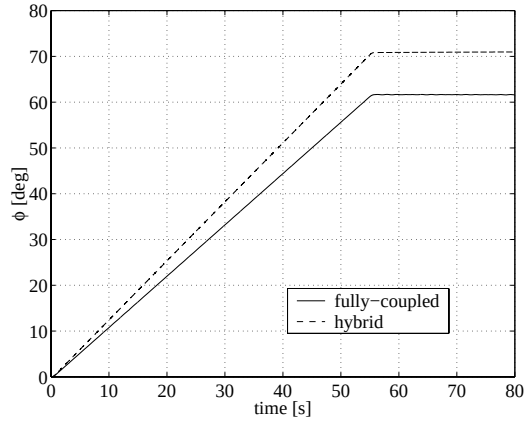

Figure 10: Example ♯2: bank angle

three pulse spin-down in $t = 5\ sec$, $t = 6\ sec$ and $t = 7\ sec$. The torque is by far lower than other examples, reaching just $1.91\ Nm$ as a maximum value, and being applied for shorter periods. Nevertheless this maneuver is interesting, because, if performed around the y_b axis, enables to highlight the limitation of the hybrid model. In fact Fig. 12 shows a divergency phenomenon occurring only for the fully-coupled model. However Fig. 15 points out that the hybrid flexible model leaves almost immediately the validity range of the linaer theory, making this comparison meaningless. Stresses on the panels for the hybrid model seems to be by far more critical than for the fully-coupled model. This discrepancy is due to an inadequacy of the hybrid model: in fact the coupling between V_x and the oscillations caused by the pitch rate q affect the C.G. motions with perturbations, which decrease the panel relative displacementes. However divergency is only delayed and a control device should be considered to stabilize the system. Once again the hybrid model turns out to

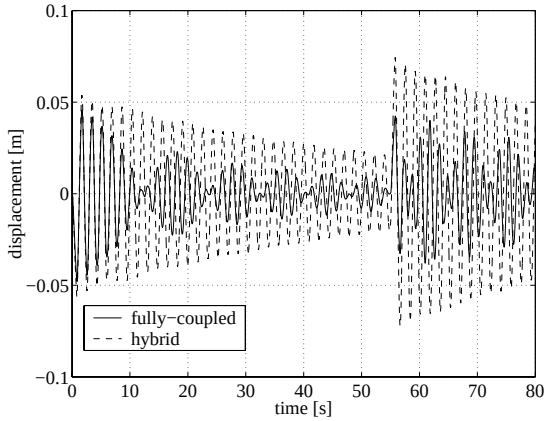

Figure 11: Example ♯2: displacement of a point on the tip panel

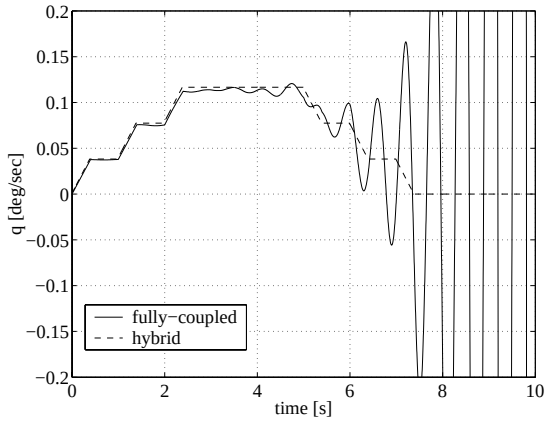

Figure 12: Example ♯3: roll rate

be conservative in the structure stress analysis, but is unreliable as far as rigid body dynamics is concerned.

Conclusions

In this paper two mathematical models for a flexible satellite were derived, with two different approaches. According to the first model, named hybrid, the equations of motion of the rigid body were written with the Newton mechanics, while flexible motion was treated with the Lagrange equations, implemented through the finite element method. In this modelization the effects of vibrations on the rigid body dyanamics are completely neglected. For the second model, named fully-coupled, the Lagrange approach is used for the overall system, enabling to evaluate the cross-coupling effects of rigid motion on flexible motion and viceversa.

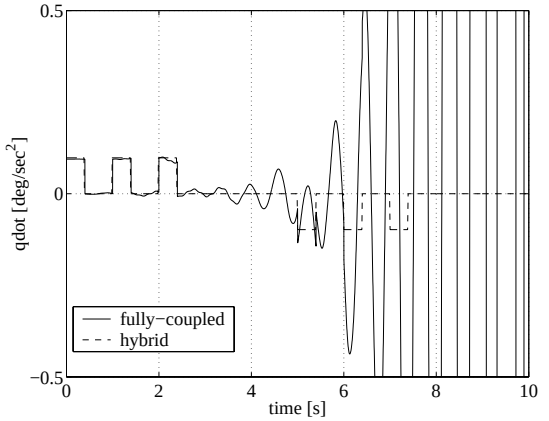

Figure 13: Example ♯3: roll accelation

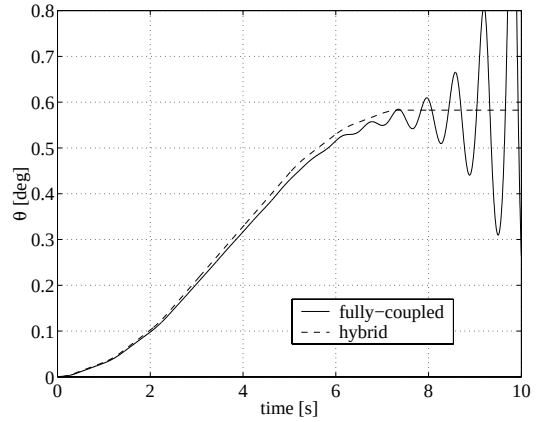

Figure 14: Example ♯3: bank angle

Results were presented in terms of time-histories of both rigid and flexible motions. They concern three examples of bang-bang maneuvers, performed with torque forcing action in the roll and pitch axes.

All the examples agree in demonstarting that the hybrid model is conservative in the estimation of the stress condition and in the forecast of a possible structure collapse. However the hybrid model is unreliable and inadequate for satellite flight dynamics and control applications, where precision and pointing requirements are particularly strict.

References

[1] Fontana, A. and Hanks, B. R., *Control of Flexible Structures (COFS) Flight Experiment Program*, Dynamics and Control of Large Structures, Proceedings of the Fifth Symposium, Blacksburg, VA, Virginia Polytechnic Institute and State University, 1985, p. 413-422.

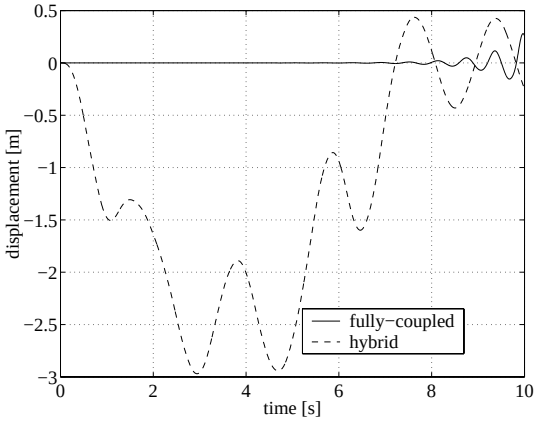

Figure 15: Example ♯3: displacement of a point on the tip panel

Table 1: First natural modes of the panels

mode	description	fn [Hz]	T [sec]
I	antisymmetric bending	0.5734	1.7422
II	antisymmetric torsion	1.6205	0.6171
III	2th antisymm. bending	3.5815	0.2792
IV	2th antisymm. tors. + hinges	5.6658	0.1765
V	3th antisymm. bending	6.0484	0.1653

[2] L. Meirovitch, H.D. Nelson, *On the High-Spin Motion of a Satellite Containing Elastic Parts* , Journal of Spacecraft and Rockets, vol. 3, Nov. 1966, pp. 1597-1602.

[3] W. Hooker, G. Margulies, *The Dynamical Attitude Equations for an n-Body Satellite* , Journal of Astronautical Sciences,vol. 12, 1965, pp. 123-128.

[4] R.E. Roberson, J. Wittemburg, *A Dynamical Formalism for an Arbitrary Number of Interconnected Rigid Bodies with Reference to the Problem of satellite Attitude Control*, Proceedings of the Third International Congress on Automatic Control, Butterworth, London, England, 1967, pp. 45D.1-46D.8.

[5] J.Y.L. Ho, R. Gluck, *Inductive Methods for Generating the Dynamic Equations of Motion for Multibodies Flexible Systems, Pt. 2, Perturbation Approach* , Synthesis of Vibrating System, ASME, New York, 1971.

[6] R.E. Roberson, *A Form of the Translational Dynamical Equations for Relative Motion in Systems of Many Non-Rigid Bodies* , Acta Mechanica, vol. 14, 1972, pp. 297-308.

[7] J.Y.L. Ho, *Direct Path Method for Flexible Multibody Spacecraft Dynamics* , Journal of Spacecraft and Rockets, vol. 14, March-April 1977, pp. 102-110.

[8] E.H. Dowell, *Free Vibration of an Arbitrary Structure in Terms of Component Modes* , Journal of Applied Mechanics, vol. 39, No. 3, 1972, pp. 727-732.

[9] L. Meirovitch, A.L. Hale, *On the Substructure Synthesis Method* , AIAA Journal, vol. 19, July 1981, pp. 940-947.

[10] E.R.Christensen, *Finite Element Analysis of Maneuvering Spacecraft Truss Structures.*, Computers and Structures, vol.32, No.6, 1989, pp. 1403-1411.

[11] R.M. Byers, S.R. Vandali, J.L. Junkins, *Near-Minimum Time, Closed-Loop Slewing of Flexible Spacecraft* , Journal of Guidance and Control, vol. 13, No. 1, 1990, pp. 57-65.

[12] W.E.Singhose, A.K.Banerjee, W.P.Seering, *Slewing Flexible Spacecraft with Deflection-Limiting Input Shaping* , Journal of Guidance, Control and Dynamics, vol.20, No.2, March-April 1997, pp. 291-298.

[13] L. Meirovitch, R.D. Quinn, *Equation of Motion for a Maneuvering Flexible Spacecraft* , Journal of Guidance, Control and Dynamics, vol. 10, No. 5, Sept.-Oct. 1987, pp. 453-465.

[14] B. Wie, *Space Vehicle Dynamics and Control* , AIAA Ed. Series, 1998, pp. 307-451.

[15] T.G. Mordfin, S.S.K. Tadikonda, M. Ruzzene, *Component Body Modeling and Controlled Articulated Flexible Multibody Dynamics* , AIAA Guidance, Navigation and Control Conference, Denver, CO, 14-17 August 2000.

[16] R.R. Bate, D.D. Mueller, J.E.White, *Fundamentals of Astrodynamics* , Dover Publications, New York, 1971.